J Mol Model (2008) 14:901–910
DOI 10.1007/s00894-008-0325-9

ORIGINAL PAPER

Cellular interaction through LewisX cluster: theoretical studies

Yun Luo · Florent Barbault · Chafika Gourmala · Yongmin Zhang · François Maurel · Yongzhou Hu · Bo Tao Fan

Received: 22 December 2007 / Accepted: 28 May 2008 / Published online: 11 July 2008

Abstract It is well known that cell surface carbohydrates play a role in cell–cell adhesion and communication. LewisX glycosphingolipids form microdomains on cell surfaces. Homotypic and calcium-mediated LewisX–LewisX (LeX-LeX) interactions were proposed to be responsible for the initial steps of cell adhesion, and to mediate embryogenesis and metastasis. Various techniques have been used to investigate such interactions, but little information is available on the geometry and the mechanism of dimerisation. To better understand these interactions, a new molecular model was developed to simulate homotypic interactions in explicit solvent with and without calcium ions. Accurate analysis of both trajectories yielded valuable information about the energetics of LeX-LeX dimerisation. Detailed interpretation of the hydrogen bond network and the presence of calcium ions along the trajectory provide valuable insights into the role of calcium ions in this carbohydrate–carbohydrate interaction.

Y. Luo · F. Barbault (✉) · C. Gourmala · F. Maurel · B. T. Fan
ITODYS, CNRS UMR 7086, Université Paris Diderot,
1 rue Guy de la Brosse,
75005 Paris, France
e-mail: florent.barbault@univ-paris-diderot.fr

Y. Luo · Y. Zhang
Laboratoire de Chimie Organique, CNRS UMR 7611,
Institut de Chimie Moléculaire (FR 2769),
Université Pierre et Marie Curie,
4 place Jussieu,
75005 Paris, France

Y. Luo · Y. Hu
ZJU-ENS Joint Laboratory of Medicinal Chemistry,
Zhejiang University,
Hangzhou 310058, China

Keywords LewisX · Molecular dynamics · Carbohydrate interactions · Carbohydrate clusters · Cellular adhesion

Introduction

Carbohydrates play vital roles in many biological processes, such as recognition, adhesion and communication between cells. Carbohydrates that are covalently linked to a non-sugar moiety (proteins, peptides or lipids) are the most prominent cell-surface-exposed structures. The highly diverse structural variability of carbohydrates makes them good candidates for cell receptors and recognition molecules. Compared to the more well known protein–protein and protein–carbohydrate interactions, carbohydrate–carbohydrate interactions are quicker and more specific, and have thus gained more and more research attention [1].

LewisX (LeX) carbohydrate is the first such carbohydrate–carbohydrate interaction to be investigated, and proved to be a homotypic and calcium-dependent interaction [2–5]. The molecule LeX-glycosphingolipid (LeX-GSL) is composed of a LewisX terminal trisaccharide unit with the carbohydrate sequence Galβ(1→4)[Fucα(1→3)] GlcNAcβ, connected to a ceramide moiety through a disaccharide lactose (Fig. 1). LeX-GSL was first identified as stage-specific embryonic antigen1′ (SSEA-1), which is highly expressed at the compaction stage of a model preimplantation embryo [6, 7]. Dramatic changes in such LeX epitopes have been observed at some steps of ontogenic development and in oncogenic transformation [8–11].

Due to the important role of LeX-GSL in cell adhesion and signal transduction, many studies have investigated the underlying molecular mechanisms, using techniques such as nuclear magnetic resonance (NMR) spectroscopy

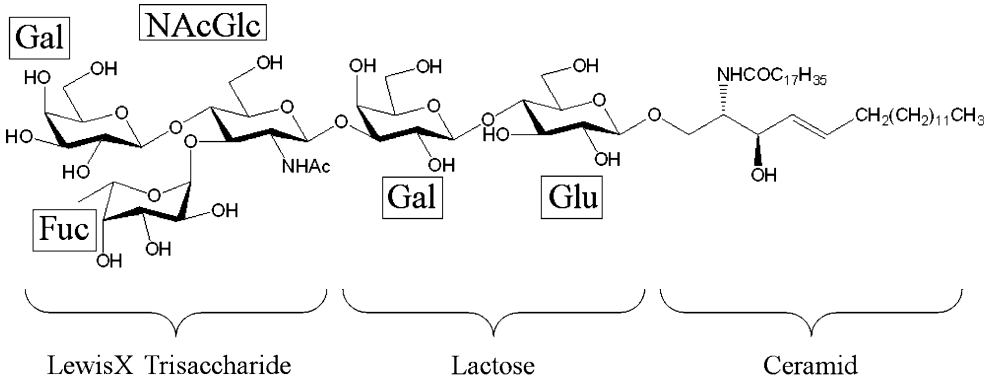

Fig. 1 Chemical structure of LewisX glycosphingolipid

[12–16], mass spectrometry (MS) [17], surface plasmon resonance (SPR) [18], vesicle adhesion [19–21], and atomic force microscopy (AFM) [22]. Rat basophilic leukaemia cells preincubated with purified LeX-GSL have also been used as a model [23]. All these approaches have contributed to the establishment of a model of calcium-ion-mediated homotypic LeX–LeX recognition. The adhesion force determined by AFM was in the range of ~20 pN for LeX trisaccharide dimerisation [14]. The adhesion energy of lipid vesicle pairs functionalised with LeX–GSL measured in $CaCl_2$ aqueous medium (0.11 M) was 67.8 μJ m^{-2} [13]. Recently, thermodynamic evidence for gold glyconanoparticles functionalised with trisaccharide LeX was obtained by isothermal titration calorimetry, providing an evaluation of binding free energy of −8.5 kcal mol^{-1} [24].

However, all applications of physical experiments are restricted by the unavailability of LeX–GSLs molecules, from either biochemical or chemical synthesis. The flexibility of carbohydrate in native solution and the inherent weakness of carbohydrate–carbohydrate interactions make experimental studies more difficult. Although the above approaches have proven the existence of calcium-ion-mediated homotypic LeX–LeX recognition, none of them has yielded any information on the dynamic geometry of the complex. In fact, the flexibility of glycosidic linkages in solution produces multiple conformations that coexist in equilibrium, and the interaction between carbohydrate molecules is a dynamic process. Nevertheless, elucidation of the conformational structures and dynamic properties of oligosaccharides is a prerequisite for a better understanding of the cell–cell adhesion and recognition process, and for the rational design of carbohydrate-derived drugs.

In the past few years, combined theoretical and experimental studies become mutually reliant in the oligosaccharide field. Computer simulation of carbohydrates in their natural environment, i.e. in water, is an important tool for molecular mechanism studies. A previous theoretical study on the tri-saccharide LeX dimer, which is a simpler molecular system, provided valuable information on the ability of LeX to form dimer [25]. This preliminary study concluded that the lactose part of the LeX molecule might play an important role in LeX–calcium recognition. The purpose of the present study was to develop a molecular dynamics (MD) model to simulate LeX–LeX interactions on cell surface microdomains, in order to better understand the mechanism of carbohydrate-dependent cell-cell interactions. The role of calcium ions in this biological process was elucidated by comparative analysis of the trajectory obtained: with and without calcium ions in the water solvent. Both trajectories yielded valuable information about the energetics of LeX–LeX dimerisation, and detailed analysis of hydrogen bonds and the presence of calcium ions along the last 2 ns trajectories provide insights into the role of calcium ions in this carbohydrate–carbohydrate interaction.

Materials and methods

Preparation of monomer coordinates

LeX pentasaccharide monomer coordinates and parameters were constructed with the "Glycam Biomolecule Builder" available online from the website of R. J. Wood group [26]. Since these coordinates are not optimised, a first minimization by molecular mechanics (1,000 steps of steepest descent followed by 1,000 steps of conjugate gradient minimization with a gradient tolerance of 0.05 kcal mol^{-1}) was made with Amber 9 [27]. This molecule was then simulated, with this software, by MD with generalised Born (GB) implicit solvent model of Hakwins et al. [28, 29] for 2 ns. Each monosaccharide unit in the LeX molecules adopts the typical $^4C_1$ chair conformation, with no significant deviation from the classical pyranose ring shape. This preliminary study was aimed at finding the most energetically favourable structure, which was found at 1,477 ps and extracted only for the atomic partial charges determination. This conformation was found with a "home-made" Perl script that merely checked all energies values, finding the lowest one and giving the associated structure.

Atomic partial charges

Molecular dynamics simulations need accurate atomic partial charges for the electrostatic energy term. The best method to obtain these, for carbohydrates systems, is to perform *ab-initio* calculations and extract the atomic charges from molecular orbitals [30]. However, this method is highly influenced by the molecular conformation. Therefore, it was decided to perform several *ab-initio* calculations from specific LeX conformations. The Random-Search method, implemented in SYBYL 7.0 [31], was used for the LeX pentasaccharide monomer to generate different conformations. Chirality checking was chosen. The energy cutoff was set to 1.0 kal/mol. The root mean square (RMS) threshold was set to 0.1 Å, with a maximum of 100 hits. The ten energetically most favourable conformations were then chosen, and their electrostatic potentials (ESP) were calculated by Gaussian 03 [32] at Hartree Fock level of calculations with the 6-31G*) basis set level. The restraint electrostatic potential method (RESP) [33] was used to obtain atomic partial charges with antechamber software, implemented in the AMBER package, for these ten structures. The values were averaged to obtain the final atomic partial charges.

Preparation of cluster coordinates

To construct a system which reflects the microenvironment of LeX–GSL microdomains on the cell surface, LeX trisaccharide packing was chosen as the referenced initial system for MD simulations. LeX trisaccharide packing was extracted from the crystallographic coordinates in the Cambridge Structural Database (code ABUCEF) [34]. The crystal structures of the LeX trisaccharide yield information related not only to the conformation of the molecule, but also to their cluster information. Along one crystal axis the trisaccharides are aligned in a row, with hydrogen bonds between fucose and galactose in neighbouring molecules (Fig. 2). The lactose moieties, which are not included in the crystal structure, were manually added using the coordinates from the energetically most favourable conformation of the pentasaccharide LeX monomer.

In reality, it is the ceramide moiety that inserts into the cell membrane and limits the linked pentasaccharide. We simplified the system by using methyl groups instead of lipid moieties, and then added the weak constraint of lactose at each side between the adjacent centre of mass of each glucose residue. Thus, the side-by-side contacts help to form clusters in order to avoid the unrealistic movement of the lactose residues. The restraint is a well with a square bottom with parabolic sides out to a defined distance, and linear sides beyond that. Restraints energy are in units of kcal/mol, and d is the distance between each adjacent centre of gravity of the glucose residues of lactose (Fig. 3). Because the distance d was found to be in the range 9–10 Å, a specific restraint potential was designed. The overall shape of this potential is represented in Fig. 4. The extremities of this potential were set at 1 Å either side of the border values (*i.e.* 8 Å and 11 Å) to allow more freedom to the cluster. In the case of a restraint violation, a square function is applied, modulating the energy for the two next Ångstoms (*i.e.* 6 Å and 13 Å); if this one moves away from this latter limit, two distinct restraints ceiling values are applied (Fig. 4). It was decided to apply a non-symmetric potential, which is energetically more constrained when the distance between adjacent residues is large (40 kcal/mol) than when this distance is small (10 kcal/mol). The reason for this asymetrical potential is that van der Waals (VdW) repulsion already represents a constraint when the adjacent residues are too close. The authors emphasise the fact that no restraint was included with the purpose of aiding LeX dimerisation, but rather to maintain cluster behaviour as it exists within the ceramide moieties.

Molecular dynamics

Two 10 ns simulations in the NPT ensemble were performed with the AMBER package version 9. The ff03 force field [27] was used for water and ions. As in a previous study [25], calcium Lennard-Jones parameters

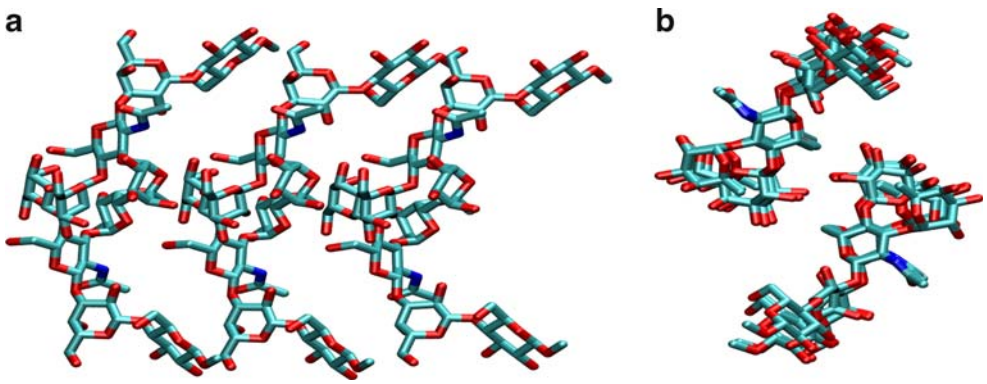

Fig. 2 Front (**a**) and side (**b**) views of the starting cluster conformation

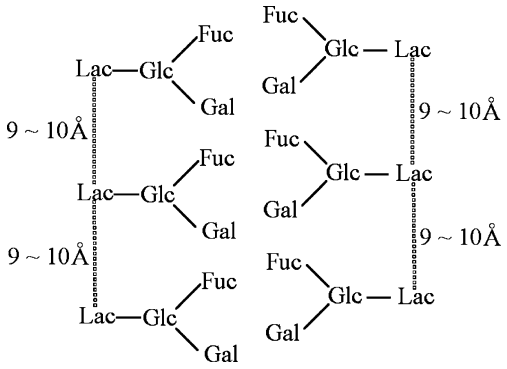

Fig. 3 Simple illustration of the six-unit packing structure with constraints

were adjusted from the Aqvist data [35] using the method defined by Bartolotti et al. [36]. The carbohydrate force field Glycam04 [37, 38] was used for all these simulations. This force field introduced to Amber all of the features necessary for carbohydrate conformational simulations, with the key focal points being treatment of glycosidic torsion angles, anomeric effects and nonbonded interactions. The TIP3P model was chosen for water. The solvent box dimension was identical for simulations with or without calcium ions: 60.3 × 55.5 × 45.0 $Å^3$. The number of water molecules was slightly different without calcium (3,466) than with ions (3,441) in order to obtain a similar solvation environment. The concentration of calcium and chloride ions was 0.16 mol/L and 0.32 mol/L, respectively. Periodic boundary conditions were applied using the particle mesh Ewald (PME) method [39] to treat long-range electrostatic interactions. Bond lengths involving bonds to hydrogen atoms were constrained using SHAKE [40]. The time step for all MD simulations was 2 fs, and a direct-space nonbonded cut-off of 8 Å was used.

In the first MD simulation, LeX packing was surrounded by water molecules. In the second MD simulation, ten calcium ions were added to the LeX packing and 20 chloride ions were also added to obtain a neutral global charge in the waterbox, which is necessary for the PME method. The starting positions of calcium ions were manually placed to distribute them uniformly around the solute, but the VdW radii of the solute. The chloride ions were moved manually to near the solvent box side such that they were as far as possible from each other and from the LeX packing. All topology and parameter files used as input for the simulations were prepared with the xleap module of AMBER. All input scripts for the MD simulations were performed with the help of the visual-AMBER software [41] developed by our team. In the two simulations, 1,000 steps of energy minimization were first performed (500 steps using the steepest descent, followed by 500 steps using the conjugate gradient algorithm). The solute atoms were frozen with strong (500 kcal/mol) harmonic restraints. The systems were then fully minimized using the same method. The systems were slowly heated from 0 to 300 K within 20 ps in the NVT ensemble. The solute and ions were kept frozen with weak atomic harmonic restraints (10 kcal/mol). Then, a 10 ns production trajectory was performed at 300 K in the NPT ensemble at 1 bar pressure and all atoms free to move. The Berendsen method [42] was used to control and adjust the temperature every picosecond. The coordinates were stored every 0.2 ps to obtain an accurate picture of molecular movement.

Analysis

The two simulations were analysed in the same way. The last 2 ns were extracted for analysis. For correct visual-

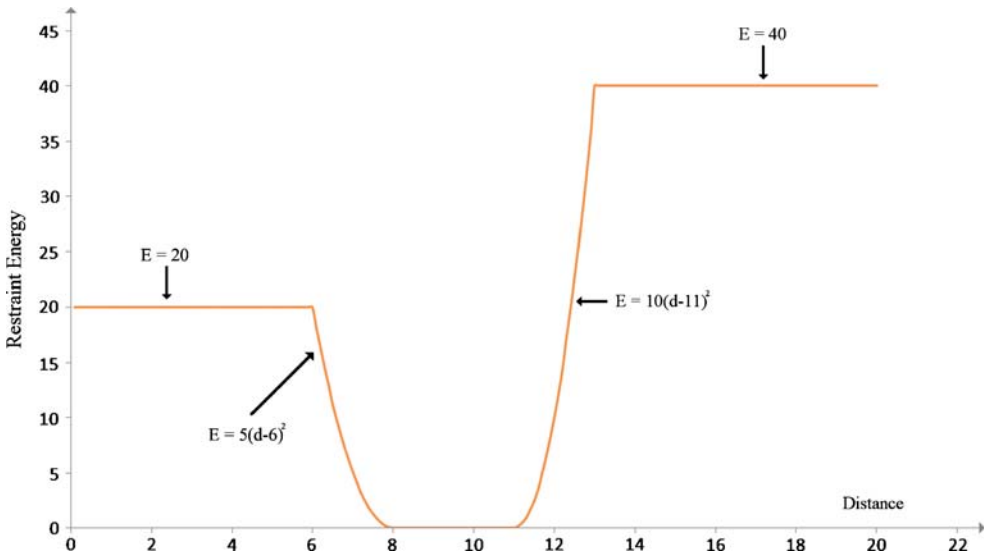

Fig. 4 Shape of the distance restraint potential energy between each adjacent glucose residue centre of mass. Energy units are in kcal/mol and distances in Ångstroms

isation, the two trajectories have been adjusted (re-imaged) in order to locate the LeX packing at the centre of the periodic boxes. VMD software [43] was used to playback trajectories resulting from MD simulations so that these trajectories can be analysed over time. All root mean square deviation (RMSD) analysis was elucidated with the Ptraj module of the Amber package. The Molecular Mechanics/Poisson-Boltzmann Surface Area (MM/PBSA) method [44–47] permits evaluation of the LeX–LeX free energy of dimerisation. The Poisson-Boltzmann (PB) equation solution was estimated with a finite-difference algorithm defined by Luo and coworkers [48], implemented in the AMBER package software. Calculations were performed to the last 2 ns with or without calcium. Snapshot solute coordinates were extracted every picosecond. The binding free energies were the averaged values of the 2,000 conformations. This energy is decomposed as follows:

$$\Delta \mathrm{G}bind = \mathrm{G}complex - \mathrm{G}lex - \mathrm{G}lex \quad \text{and}$$

$$\Delta \mathrm{G}bind = \Delta \mathrm{Egas} + \Delta \mathrm{G}sol - \mathrm{T}\Delta \mathrm{S}gas$$

$$\Delta Egas = \Delta Eint + \Delta Eelec + \Delta Evdw$$

$$\Delta Gsol = \Delta Gpolar + \Delta Gnp$$

$$\Delta Sgas = \Delta Strans + \Delta Srot + \Delta Svib$$

The sum of the molecular mechanics energy, ΔEgas, is divided into three parts: internal energy (ΔEint), electrostatic potential (ΔEelec) and van der Waals (ΔEvdw) potential. The solvation free energy (ΔGsol) is composed of two parts: polar solvation free energy (ΔGpolar) and non-polar solvation free energy (ΔGnp). The polar term was calculated using a numerical solver for the PB method or by GB methods. ΔGnp was determined using the MOLSURF method [49]. The latter is directly related to the solvation-accessible surface area (SASA) [50]:

$$\Delta \mathrm{Gnp} = \mathrm{Surften} \times \mathrm{SASA} + \mathrm{Surfoff}$$

Surften (surface tension) and Surfoff are constants equal to 0.0052 and 0.92, respectively. The solute entropy is estimated with normal mode analysis by computing the contributions of translation, rotation and vibration. This analysis is done with Amber 9 and requires accurate minimizations, therefore each snapshot was optimized with 5×10^5 steps and an RMS convergence of 0.001 kcal. A SASA calculation was used to determine the random probability of the presence of an interacting ion with each residue. To obtain this value easily, the Surften and Surfoff constants from the previous equation were set to 1 and 0, respectively. Energy decomposition was computed and, consequently, ΔGnp directly represents the SASA value. The solvent accessible surface of the entire residue (SASAmax) was calculated with isolated residues by MOLMOL 2k.2.0 [51] using the CalcSurface command as a reference to evaluate the percentage of hidden surface. The ptraj program in Amber 9 contains a facility for keeping track of lists of pair interactions between a list of hydrogen bond donors and hydrogen bond acceptors for calculations of hydrogen bonding. A hydrogen bond was considered to be present when the donor–acceptor distance is smaller than 3.5 Å and the donor–acceptor angle is smaller than 60°. These weak criteria were chosen deliberately to count as much hydrogen bonding information as possible.

Results and discussion

Overall cluster analysis

Monitoring of kinetic, potential and overall energies along the trajectory, as well as the pressure and temperature, indicates that both systems are stable. The restraint energy was recorded along both trajectories. No large variation was observed and the energy value was always below 3 kcal/mol, which means that the restraints are in agreement with the molecular system and are present only to maintain the cluster system. The global RMSD of both systems show that the systems present high flexibility (Fig. 5). The central dimer is the more important because the systems considered present the smallest possible cluster and there are "end-side effects" with the solvent for residues other than the central dimer.

Overall dimer analysis

The RMSD for the central dimer is stable, showing that the system is stable and that the analysis can be performed for the last 2 ns (Fig. 6). The system without calcium ions was equilibrated after 2.2 ns, and the system with calcium ion was equilibrated more quickly, *i.e.* after 1ns. Visual examination of the two 10 ns trajectories shows that is no chelating complex with Ca^{2+} observed, and the dimer is maintained with or without calcium ions. These observations are in agreement with previous experimental studies [6, 9, 15, 16]. Moreover, no specific hydration pattern was observed for the central dimer in the presence or absence of calcium ions.

The average structure is different, and Ca^{2+} induced a slight but significative influence on the structure of the LeX–LeX adhesion. In addition, the RMSD fluctuations illustrated in Fig. 6 indicate that the flexibility of this carbohydrate system is moderate, and is similar with or without calcium ions. The RMSD for each residue (not shown here), with or without Ca^{2+}, shows no significant variation, meaning that calcium ions have no significant impact on the local movements of specific LeX residues.

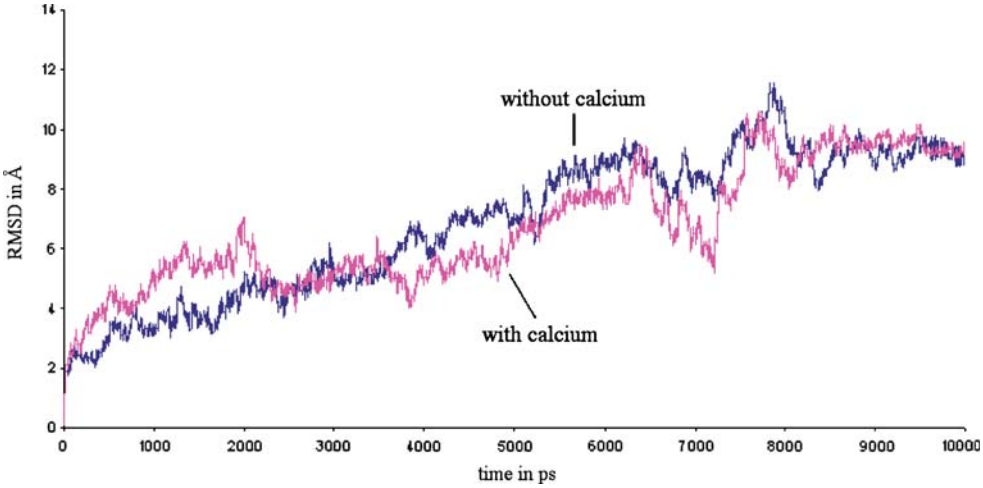

Fig. 5 Ten-nanosecond root mean square deviation (RMSD) for the whole cluster

Free energy

The calculated free energies of binding are negative both in the presence or absence of calcium (Table 1), which is in agreement with previous related experiments. The results show that calcium seems to be favourable for the dimerisation of LeX, with a decrease in free energy from −4.0 kcal/mol to −10.0 kcal/mol (PB), and from −1.7 kcal/mol to −8.3 kcal/mol (GB). The electrostatic part and the VdW contribution are more important, which is in agreement with a cation influence. The values of the electrostatic part and the VdW contribution in the system with calcium ions are lower than without ions. This indicates that there is some specificity for calcium ions. The solute entropic contribution is not significant for the selectivity. Our free energy value (−10.0 kcal/mol with the PB method and −8.3 kcal/mol with the GB method) for the LeX pentasaccharide dimer with calcium ions is closely comparable to the experimental value (−8.5 kcal/mol) obtained for the LeX trisaccharide dimer with calcium [24]. This good correlation between the simulation and experimental results is a strong indication of the accuracy of our simulations.

Hydrogen bonds

There are 14 hydroxyl groups and one acetyl amino group in each LeX pentasaccharide and, as the systems are in an aqueous environment, the hydrogen bond appears to have an especially significant role in the control of structure and biological function. The concept of hydrogen bonding certainly provided a key to understanding carbohydrate–carbohydrate interaction. Figure 7 displays the hydrogen bonding network of the middle dimer on both trajectories, and the average presence of each hydrogen bond during the trajectory of the final 2 ns (only values >20% are shown).

There are more hydrogen bonds in the system with Ca^{2+} than that without ions, thus the cation has a positive influence on the system leading to the formation of hydrogen bonds. We classified the hydrogen bonds into two distinct classes: intra- and inter-monomers. Both trajectories, with and without Ca^{2+}, display the same number of intra-monomer hydrogen bonds. They involve the same atoms and, more or less, the same percentage of presence. This indicates that the calcium ions do not induce a modification of the LeX monomer structure and stability.

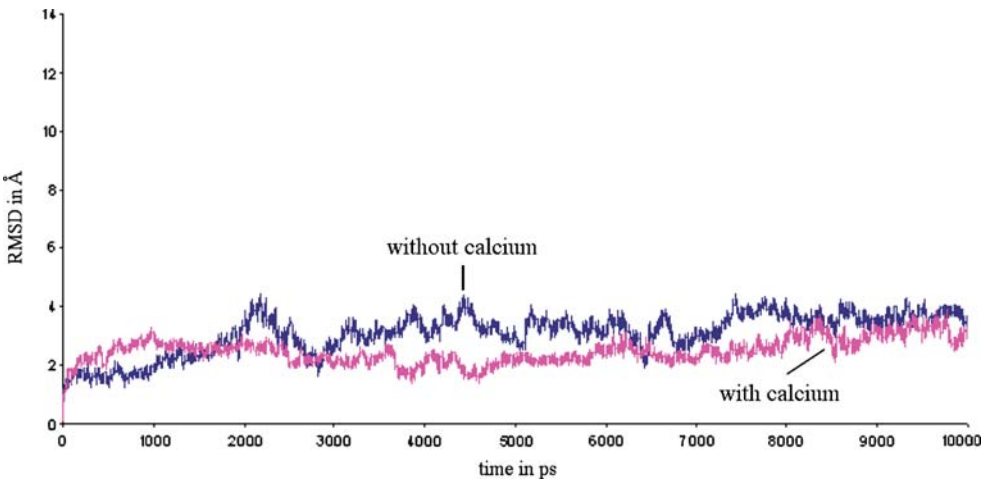

Fig. 6 Ten-nanosecond RMSD for the central dimer indicating stability of the system and the moderate flexibility of the dimer

Table 1 Free energy (in kcal/mol) analysis performed with molecular mechanics/Poisson-Boltzmann surface area (MMPBSA) and molecular mechanics/generalised Born surface area (MMGBSA) for the final 2 ns

Contributions	With Ca^{2+}	Without Ca^{2+}	Delta
ELE	−19.7±3.8	−8.5±3.2	−11.2
VDW	−12.8±2.4	−8.7±2.7	−4.1
G non-elec	−2.3±0.10	−1.5±0.12	−0.8
G elec (PB)	24.5±2.2	15.3±2.1	9.2
G elec(GB)	26.2±3.1	17.6±2.9	8.6
T.Strans	−8.8±0.0	−8.8±0.0	0.0
T.Srot	−5.7±0.2	−5.5±0.3	−0.2
T.Svib	14.2±3.1	14.9±3.4	−0.7
ΔG (PB)	−10.0±1.9	−4.0±1.1	−6.0
ΔG (GB)	−8.3±1.4	−1.7±1.7	−6.6

The inter-monomer hydrogen bonds are more important for studying dimerisation. The most interesting change is that the number of interactions are different with four hydrogen bonds in the presence of calcium compared to two hydrogen bonds without these ions (Fig. 7). This may explain the difference in dimerisation free energies and therefore the positive influence of the calcium ions that prescribe the presence of these hydrogen bonds. Among these interesting interactions, we note the very strong hydrogen bond between the O_2 of the galactose residue in each monomer that is observed at 97% presence in the system with calcium, but which is absent when there is no ion in the system. Similarly, another strong hydrogen bond (75%) is observed only in the presence of calcium and involves the 3′-OH group of the galactose residue of the lactose moiety with the facing 6′ hydroxyl group of the residue N-acetyl glucosamine. This latter hydroxyl group is also implicated in a less important inter-monomer hydrogen bond (21%) with the 3′ hydroxyl fucose group. The OH-4′ in the same galactose residue was also very important as it participated as a hydrogen bond acceptor in systems both with and without calcium ions.

Calcium interaction

The positions of calcium ions along the trajectory were monitored to investigate the electrostatic interactions of the LeX dimer with cations. Representation of calcium ions along the trajectory shows that calcium takes up specific preferred positions along the trajectory (Fig. 8). The percentage of presence of calcium ions is calculated for every residue of the central dimer (Table 2). The proximity of calcium to each residue is considered when its distance from the centre of mass of each residue is less than 10 Å. The OCH_3 group is here only to mimic the ceramide moiety, but it is too small. Therefore, we cannot draw any conclusions about the Ca^{2+} presence for this residue. The chloride ions move a lot within the periodic box, and no noticeable interactions were recorded. The RMSD of the anion is 77.7 ± 27 Å, which is, indubitably, high and indicates that these ions are free to move within the box.

For each residue, it is important to look at the solvent accessibility surface area (SASA). A SASA calculation was used to determine the random probability of the presence of an interacting calcium ion with each residue. If all the SASA of each residue corresponds to the presence of calcium, that means calcium ions are just randomly distributed around each residue. In that case, the different presence of ions has no relationship with any special

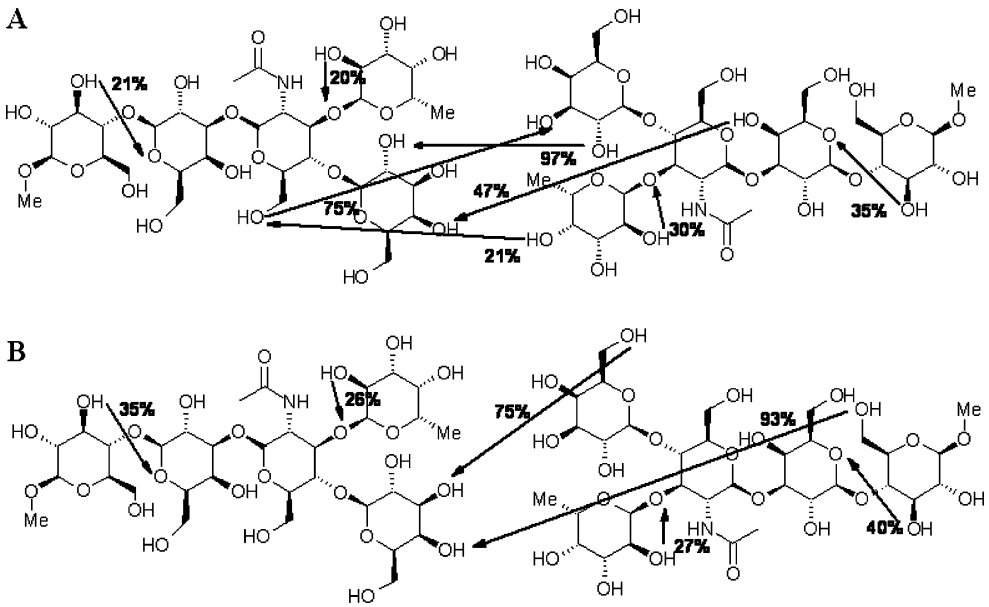

Fig. 7 **A**,**B** Hydrogen bond network. **A** With calcium ions, **B** without calcium ions. The percentage values indicate the time of presence (along the 2 ns analysis) of these hydrogen bonds. Only bonds that are present more than 20% of the time are displayed on these schemes

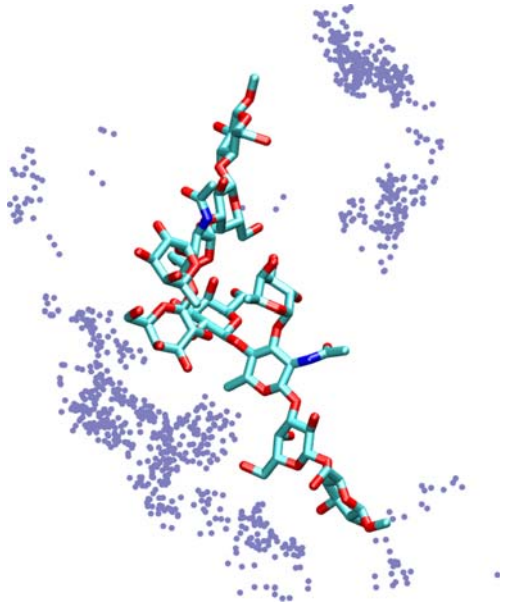

Fig. 8 Calcium population density around the LewisX carbohydrate (after the trajectory has been fitted to the primary unit cell). All central dimer coordinates are fitted along the time axis, whereas calcium ion positions are recorded and represented as points. The clouds of points indicate that the ions are not randomly placed around the dimer but take up preferred positions

interaction with certain residues, so there is no real interaction with carbohydrate. The percentage hidden for each residue is defined by the formula:

$$\%\text{Hidden} = (1 - \text{SASA}/\text{SASAmax}) \times 100\%.$$

A linear correlation between the "hidden percentage" and the presence percentage of calcium was attempted (data not shown) and has led to an R square value of 0.141, indicating that there is no correlation between accessibility and presence percentage for calcium (Fig. 9). This proves that calcium comes near certain residues because of specific recognition.

In order to gain a deeper insight into the specificity of the calcium ions, an atomic calcium percentage of presence was calculated with the same definition (values reported in Fig. 10). It should be pointed out that the hydroxyl groups do not exhibit similar behaviour towards calcium ions. Logically, hydroxyl groups engaged in hydrogen bonds interact rarely with calcium. The groups displaying a percentage of presence higher than 20% indicate a strong specific interaction with the cations, as indicated with grey colour in Fig. 10. Note that two distinct continuous areas display a strong interaction with calcium. The first (Fig. 10b) concerns the lactose moiety of this glycosphingolipid, with atoms O5′, O1′, O2′, O3′ and O4′ of the glucose residue, and atoms O5′ and O6′ from galactose. A role for the lactose moiety towards the calcium cation was previously proposed [25]; this study confirms this proposition. The second area (Fig. 10a) implicates the tri-saccharide part of LeX and contains the oxygen atoms O1′, O4′, O5′ and O6′ of the galactose residue; the oxygen atoms O1′, O2′ and O3′ of the fucose residue, and O5′ and O6′ of N-acetyl glucosamine. This specificity of calcium for this LeX tri-saccharide has also been proved in several experimental studied [3, 14, 17, 19–21, 23, 24]. However, none of these latter works was able to determine which oxygen atoms were involved in specific calcium recognition. This work is thus the first to propose this list of oxygen atoms.

Conclusions

Cell surfaces are rich in carbohydrates, which are assumed to be involved in cell recognition and adhesion. This is currently a major theme in cell biology. This work represents a theoretical study of LewisX glycosphingolipid dimerisation in a carbohydrate cluster built by experimental

Table 2 Solvent accessible surface area (SASA), calcium ion presence and surface hidden percent of each residue

	Residue	SASA	$SASA_{max}$	$\%Ca^{2+}$	%Hidden[a]
Monomer 1	OMe	95.3±2.4	160.0	33.6	40.4
	Glu	196.5±5.9	340.9	27.2	42.4
	Gal	171.2±8.0	340.2	13.5	49.7
	NAcGlc	204.3±5.3	405.4	10.7	49.6
	Fuc	186.9±5.0	331.2	10.4	43.6
	Gal	217.2±4.9	340.6	19.7	36.2
Monomer 2	OMe	93.8±2.6	160.0	26.0	41.4
	Glu	198.2±4.7	340.9	21.3	41.9
	Gal	167.2±6.6	340.2	20.1	50.9
	NAcGlc	208.2±4.5	405.4	14.9	48.6
	Fuc	189.4±6.0	331.2	9.8	42.8
	Gal	220.6±3.9	340.6	17.9	35.2

[a] %Hidden=(1− SASA/SASAmax) ×100%

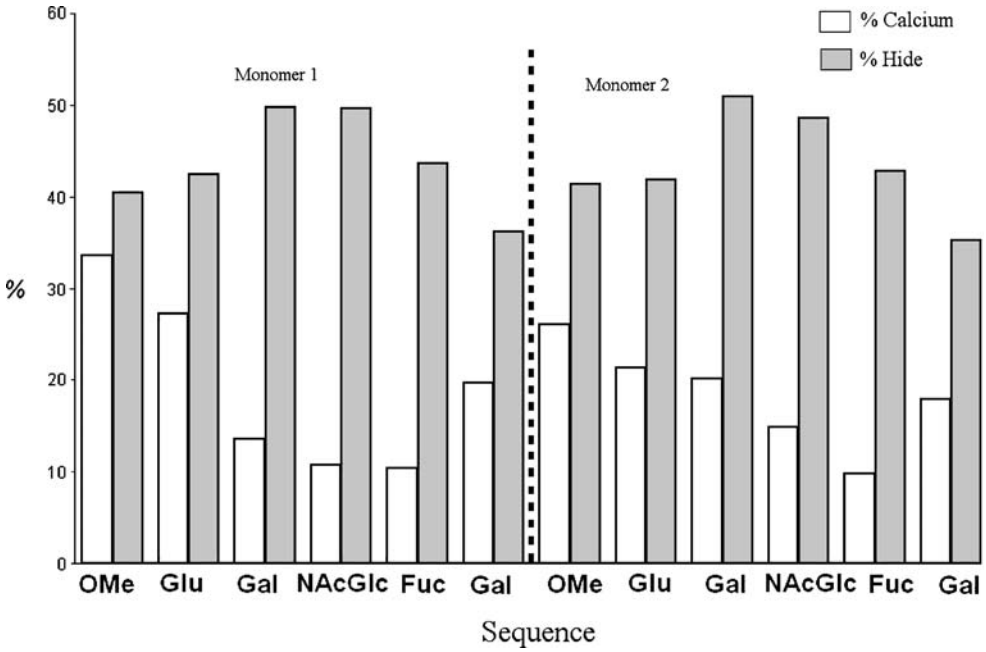

Fig. 9 Histogram of calcium presence and solvent hide percentages

crystallographic packing. Two 10 ns of molecular dynamics simulations were conducted in the presence or in the absence of calcium ions. Due to border effects, only the central dimer was examined. This dimer is stable in both the presence and absence of calcium cations, which is in agreement with much experimental data. Free energy calculations were estimated with the MMPB(GB)SA method and the values obtained indicate that calcium ions significantly increase the stability of the LeX dimer. Hydrogen bonding networks recorded over time displayed different patterns with or without calcium, which may explain the observed stability variations. According to this analysis, some specific hydroxyl groups in the dimerisation process were elucidated. Positions of calcium ions along the trajectory were monitored to investigate the interactions of this ion with the LeX dimer. An original calculation of hiding percent indicates that there is no correlation with calcium proximity, leading us to conclude that calcium ions are not randomly placed around the dimer but exhibit real specificity. A more detailed analysis of calcium positions indicated that two continuous areas of LeX atoms interact strongly with this ion. These areas were located to the trisaccharide and lactose moeities of LeX. This study is the first to present a list of atoms that are expected to be involved in calcium recognition. Several chemical synthesis of specific deoxy-LeX have been made [52–54], or are in progress, in order to verify these atomic roles experimentally. It should be pointed out that this model concerns only a few molecules, in comparison to a cellular glycosphingolipid raft where some molecular interactions might be slightly different. Consequently, and in order to increase the accuracy of the model, new molecular dynamics simulations will be launched with a bigger cluster model. These structures, called glycolandscapes, have already been studied [55] and prove the feasibility of such models. Several diseases processed, such as tetratocarcinoma F9, use LeX cellular adhesion for their autoaggregation. The elucidation of such structure–function relationships is expected to lead to new ideas and methods for the prevention and cure of those specific diseases.

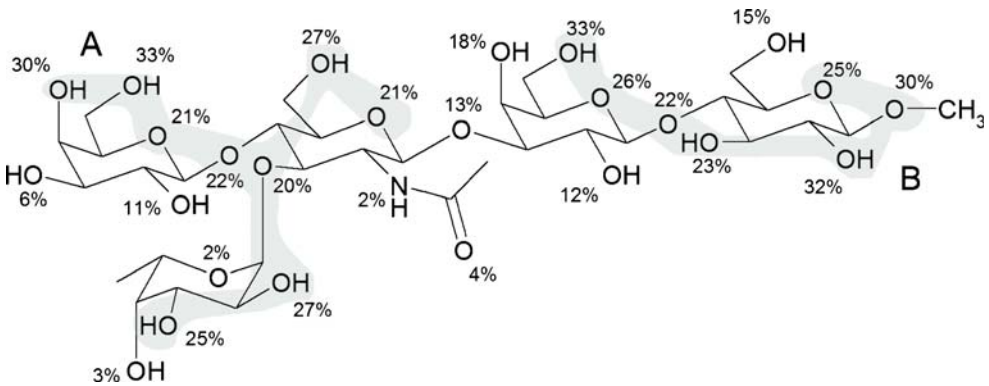

Fig. 10 Calcium percentage of time presence. Hydroxyl groups display different behavior with calcium ions. Two distinct continuous areas of high atomic affinities (more than 20%), **A** and **B**, are showed in *grey*

Acknowledgements We are indebted to Paris–Diderot University and the French embassy in China for the award of a PhD fellowship to Yun Luo. This work is dedicated to the memory of Professor BoTao Fan, who died on 22 October 2006, who initiated and led this project.

References

1. Mammen M, Choi S-K, Whitesides GM (1998) Angew Chem Int Ed 37:2754–2794
2. Dwek RA (1996) Chem Rev 96:683–720
3. Eggens I, Fenderson B, Toyokuni T, Dean B, Stroud M, Hakomori S (1989) J Biol Chem 264:9476–9484
4. Hakomori S (1996) Cancer Res 56:5309–5318
5. Kojima N, Fenderson BA, Stroud MR, Goldberg RI, Habermann R, Toyokuni T, Hakomori S (1994) Glycoconj J 11:238–248
6. Kannagi R, Nudelman E, Levery SB, Hakomori S (1982) J Biol Chem 257:14865–14874
7. Solter D, Knowles BB (1978) Proc Natl Acad Sci USA 75:5565–5569
8. Hakomori S, Nudelman E, Levery SB, Kannagi R (1984) J Biol Chem 259:4672–4680
9. Singhal AK, Orntoft TF, Nudelman E, Nance S, Schibig L, Stroud MR, Clausen H, Hakomori S (1990) Cancer Res 50:1375–1380
10. Yang HJ, Hakomori SI (1971) J Biol Chem 246:1192–1200
11. Yuan M, Itzkowitz SH, Ferrell LD, Fukushi Y, Palekar A, Hakomori S, Kim YS (1987) J Natl Cancer Inst 78:479–488
12. Gege C, Geyer A, Schmidt RR (2002) Eur J Org Chem 2002:2475–2485
13. Geyer A, Gege C, Schmidt RR (1999) Angew Chem Int Ed 38:1466–1468
14. Geyer A, Gege C, Schmidt RR (2000) Angew Chem Int Ed 39:3245–3249
15. Henry B, Desvaux H, Pristchepa M, Berthault P, Zhang YM, Mallet JM, Esnault J, Sinay P (1999) Carbohydr Res 315:48–62
16. Wormald MR, Edge CJ, Dwek RA (1991) Biochem Biophys Res Commun 180:1214–1221
17. Siuzdak G, Ichikawa Y, Caufield TJ, Munoz B, Wong C-H, Nicolaou KC (1993) J Am Chem Soc 115:2877–2881
18. Hernaiz MJ, de la Fuente JM, Barrientos AG, Penades S (2002) Angew Chem Int Ed 41:1554–1557
19. Gourier C, Pincet F, Perez E, Zhang Y, Mallet JM, Sinay P (2004) Glycoconj J 21:165–174
20. Gourier C, Pincet F, Perez E, Zhang Y, Zhu Z, Mallet JM, Sinay P (2005) Angew Chem Int Ed 44:1683–1687
21. Pincet F, Le Bouar T, Zhang Y, Esnault J, Mallet JM, Perez E, Sinay P (2001) Biophys J 80:1354–1358
22. Tromas C, Rojo J, de la Fuente JM, Barrientos AG, Garcia R, Penades S (2001) Angew Chem Int Ed 40:3252–3255
23. Boubelik M, Floryk D, Bohata J, Draberova L, Macak J, Smid F, Draber P (1998) Glycobiology 8:139–146
24. de la Fuente JM, Eaton P, Barrientos AG, Menendez M, Penades S (2005) J Am Chem Soc 127:6192–6197
25. Gourmala C, Luo Y, Barbault F, Zhang Y, Ghalem S, Maurel F, Fan BT (2007) J Mol Struct Theochem 821:22–29
26. Woods RJ, Dwek RA, Edge CJ, Fraser-Reid B. Glycam Biomolecule Builder http://www.glycam.com/CCRC/biombuilder/biomb_index.jsp
27. Case D, Darden T, Cheatham T, Simmerling C, Wang J, Duke R, Luo R, Merz K, Pearlman D, Crowley M, Walker R, Zhang W, Wang B, Hayik S, Roitberg A, Seabra G, Wong K, Paesani F, Wu X, Brozell S, Tsui V, Gohlke H, Yang L, Tan C, Mongan J, Hornak V, Cui G, Beroza P, Mathews D, Schafmeister C, Ross W, Kollman P (2006) AMBER University of California
28. Hawkins GD, Cramer CJ, Truhlar DG (1996) J Phys Chem 100:1578–1599
29. Tsui V, Case DA (2001) Biopolymers 56:275–291
30. Cieplak P, Cornell WD, Bayly C, Kollman PA (1995) J Comp Chem 16:1357–1377
31. SYBYL Tripos, http://www.tripos.com
32. Frisch MJ, Trucks GW, Schlegel HB, Scuseria GE, Robb MA, Cheesman JR, Montgomery JAJ, Vreven T, Kudin KN, Burant JC, Millam JM, Iyengar SS, Tomasi J, Barone V, Mennuci B, Cossi M, Scalmani G, Rega N, Pertesson GA, Nakatsuji H, Hada M, Ehara M, Toyota K, Fukuda R, Hasegawa J, Ishida M, Nakajima T, Honda Y, Kitao O, Nakai H, Klene M, Li X, Knox JE, Hratchian HP, Cross JB, Bakken V, Adamo C, Jamarillo J, Gomperts R, Stratmann RE, Yazyev O, Austin AJ, Cammi R, Pomelli C, Ochterski JW, Ayala PY, Morokuma K, Voth GA, Salvador P, Dannenberg JJ, Zakrzewski VG, Dapprich S, Daniels AD, Strain MC, Farkas O, Malick DK, Rabuck AD, Raghavachri K, Foresman JB, Ortiz JV, Cui Q, Baboul AG, Clifford S, Cioslowski J, Stefanov BB, Liu G, LIashenko A, Piskorz P, Komaromi I, Martin RL, Fox DJ, Keith T, Al-Laham MA, Peng CY, Nanayakkara A, Challacombe M, Gill PMW, Johnson B, Chen W, Wong MW, Gonzalez C, Pople JA (2004) Gaussian 03, Revision C.02. Gaussian, Wallingford, CT
33. Bayly C, Cieplak P, Cornell WD, Kollman PA (1993) J Phys Chem 97:10269–10272
34. Perez S, Mouhous-Riou N, Nifant'ev NE, Tsvetkov YE, Bachet B, Imberty A (1996) Glycobiology 6:537–542
35. Aqvist J (1990) J Phys Chem 94:8021–8024
36. Bartolotti LJ, Pedersen LG, Charifson PS (1991) J Comp Chem 12:1125–1128
37. Kirschner KN, Woods RJ (2001) Proc Natl Acad Sci USA 98:10541–10545
38. Woods RJ, Dwek RA, Edge CJ, Fraser-Reid B (1995) J Phys Chem 99:3832–3846
39. Darden T, York D, Pedersen L (1993) J Chem Phys 98:10089–10092
40. Ryckaert JP, Ciccotti G, Berendsen HJC (1977) J Comput Phys 23:327–341
41. Barbault F, Gourmala C, Zhang Y, Ghalem S, Fan BT (2005) CMTPI, Shanghai
42. Berendsen HJC, Postma JPM, van Gusteren WF (1984) J Chem Phys 81:3684–3690
43. Humphrey W, Dalke A, Schulten K (1996) J Mol Graph 14:33–38
44. Kollman PA, Massova I, Reyes C, Kuhn B, Huo S, Chong L, Lee M, Lee T, Duan Y, Wang W, Donini O, Cieplak P, Srinivasan J, Case DA, Cheatham TE 3rd (2000) Acc Chem Res 33:889–897
45. Massova I, Kollman PA (1999) J Am Chem Soc 121:8133–8143
46. Wang J, Morin P, Wang W, Kollman PA (2001) J Am Chem Soc 123:5221–5230
47. Wang W, Kollman PA (2001) Proc Natl Acad Sci USA 98:14937–14942
48. Luo R, David L, Gilson MK (2002) J Comp Chem 23:1244–1253
49. Sitkoff D, Sharp KA, Honig B (1994) Biophys Chem 51:397–403, see discussion pp 404–399
50. Sitkoff D, Lockhart DJ, Sharp KA, Honig B (1994) Biophys J 67:2251–2260
51. Koradi R, Billeter M, Wuthrich K (1996) J Mol Graph 14:51–55, 29–32
52. Gourmala C, Zhu Z, Luo Y, Fan BT, Ghalem S, Hu Y, Zhang Y (2005) Tetrahedron Asymmetry 16:3024–3029
53. Luo Y, Dong D, Barbault F, Fan BT, Hu Y, Zhang Y (2008) C R Chimie 11:29–37
54. Luo Y, Gourmala C, Dong D, Barbault F, Fan BT, Hu YZ, Zhang Y (2008) Glycoconj J (25:335–344), doi:10.1007/s10719-10007-19077-10715
55. Imberty A, Breton C, Oriol R, Mollicone R, Perez S (2003) Adv Macromol Carbohydr Res 2:67–130